Thiourea dioxide as a green reductant for the mass production of solution-based graphene

Yanqing Wang, Ling Sun, Bunshi Fugetsu*

Nano-Technology Industrialization Laboratory, Graduate School of Environmental Science, Hokkaido University, Sapporo 060-0810, Japan

Abstract

Mass production of solution-based graphene derived from the precursor graphene oxide is a challenging step toward achieving industrialization of graphene. Inspired by a classical reducing method performed in the textile and paper making industries, we report here a rapid, cost-effective and safer approach to the facile production of graphene that employs thiourea dioxide (TDO) as the green reductant. Graphene oxide was converted into high quality graphene within 30 minutes with TDO as the reductant under moderate reaction conditions. The C/O ratio of the TDO reduced graphene was ~5.9 with the yield of graphene from graphene oxide > 99%. This is better than the reduction efficiency under the identical experimental conditions by using L-ascorbic acid as the reductant which required a reaction time of about 48 hours. This simple and effective procedure should offer an alternative route to the mass production of solution-based graphene for practical applications.

1. Introduction

Graphene, a novel two-dimensional structure patterned with sp^2 bonded carbon atoms, has been the subject of intense study due to its unique morphologies and attractive properties [1-3]. In fact, graphene is the thinnest sheet-shaped molecule with an ultra-large surface area and superior mechanical and electronic properties [4] and holds great promise in applications in electronic devices, sensors, electrodes, and the other graphene-based composite materials. Large scale production of high quality graphene has been the key to achieving the goal of graphene industrialization [5]. Methods such as chemical vapor deposition (CVD) of hydrocarbons on transition metal substrates and epitaxial growth via high temperature treatment of silicon carbide are capable of producing high quality graphene, but these methods are difficult to scale up. The solution-based chemical oxidation of graphite has long been used for the mass production of graphene oxide, a solution-based precursor of graphene. However, a reduction step is required to convert the graphene oxide into graphene. Chemical reduction was commonly used and this was achieved with hydrazine and/or its derivatives [6-11], hydroquinone[12], $NaBH_4$ [13-16], sodium hydrosulfite[17], L-ascorbic acid[18-20], amino acid[20], carrot root [21], pyrrole[22], and thiourea [23] as the typical reductants. The so-called thermal reduction [24], microwave irradiation reduction [25], and electrochemical reduction [26] were also applied to this procedure. Hydrazine or hydrazine hydrate have been used extensively due to their strong reducing capabilities, however, C-N groups were incorporated during the reduction reaction and remained in the resulting graphene, lowering the quality of the product. Furthermore, hydrazine is toxic in nature and also highly explosive and its use should be avoided, especially in reactions that require large scale implementation. In an effort to replace hydrazine, sodium borohydride ($NaBH_4$) was used, but this reductant is readily hydrolyzed and gave rise to an unstable aqueous solution, resulting in low efficiency in the reduction. Other chemically safe reducing agents, such as amino

acids, carrot root, and pyrrole showed some abilities to reduce graphene oxide into graphene, but their reduction potential was far inferior to that of hydrazine. L-Ascorbic acid (vitamin C), the so-called green reductant, showed a higher ability for reducing graphene oxide into graphene; however, the reducing procedure was rather complicated and time-consuming (requiring around 48 hours).

Graphene oxide possesses a chemical structure that is similar to that of the so-called vat dyes which have long been used in the textile and paper industry. As shown in Figure 1, graphene oxide can be described as a random distribution of oxidized areas with oxygen-containing functional groups combined with non-oxidized regions where most of the carbon atoms preserve their sp^2 hybridization[5, 15, 27-29]. In this study, inspired by the widespread use of this reductant in the dyeing process of treating cellulosic fibers with vat dyes in the textile and paper making industries, thiourea dioxide (TDO, formamidine sulfinic acid) is used to reduce graphene oxide into graphene. TDO appears terrifically stable in 20 - 30 °C in solution, but when it is heated or catalyzed by alkali, it decomposes rapidly to produce sulfoxylic acid through formamidine sulfinic acid to act as a strong reductant. We demonstrate in this study that TDO, a traditional yet green reductant, is a highly capable species for chemical reduction of graphene oxide into graphene of high quality. To our best knowledge, this is the first paper reporting the use of TDO as a green reductant for the mass production of high quality solution-based graphene.

2. Experimental

2.1 Preparation of graphene oxide

Graphene oxide was obtained from expanded graphite, based on the method proposed by Hummers and Offeman [30]. In a typical treatment, 5 g of the expanded graphite was dispersed in 115 ml concentrated sulfuric acid in an ice bath. Approximately 5 g sodium nitrate and 15 g potassium

permanganate were slowly added to the chilled mixture, cooled by an ice bath, and stirring was continued for 2 hours. The mixture gradually became pasty and blackish-green. Then, the mixture was placed in a 35 °C water bath and kept at that temperature for 30 min, followed by the slow addition of distilled water (500 ml) to keep the solution from effervescing. The resulting solution was placed at well below 98 °C for 2 hours. As the reaction progressed, the color of the mixture turned yellowish. The mixture was further treated with 5% H_2O_2 (200 ml), filtered and washed with distilled water several times until its supernatant was without SO_4^{2-}, as tested by barium chloride solution (0.2 mM). The purified graphene oxide was finally dispersed in water and ultrasonically exfoliated in an ultrasonic bath for 1 hours to form a stable graphene oxide aqueous dispersion.

2.2 Reduction of graphene oxide using TDO

The solution based graphene was prepared by adding 2.5 g TDO into 100 mL graphene oxide aqueous solution (pH 9.0; 0.2wt%) at 80 ºC for 30 min; sodium cholate was used as a stabilizer to maintain the TDO-reduced graphene with high stability in the aqueous solution. For preparing the TDO-reduced films, the graphene oxide film was firstly prepared on glass-based substrates through the dropping method and then dried at 80 ºC in an oven. The graphene oxide-based films were immersed in the reducing agent aqueous solution containing 25 mg mL^{-1} of TDO and adjusted to pH 9.0 using NaOH solution (1.0 wt%), followed by a reduction reaction of 30 min in 80 °C. The color of the films changed from yellow-brown to metallic gray. Finally, the obtained graphene films were washed using distilled water to remove the by-product (urea and sodium sulfite) and the residual reducing agents, and then dried at 80 ºC in an oven. Graphene obtained using sodium hydrosulfite and L-ascorbic acid as reductants were also prepared, for the comparison studies.

2.3 Characterizations

Atomic force microscopy (AFM) images were acquired using an Agilent Series 5500 AFM instrument. The samples were prepared by casting a highly diluted aqueous graphene oxide aqueous suspension on the surfaces of mica. The images were obtained using the tapping mode at a scanning rate of 0.5 Hz. The X-ray diffraction (XRD) measurements were performed with a Rigaku RINT Ultima diffractometer with Cu-Kα radiation (Kα 1.54056 Å) and an X-ray power of 40 kV/20 mA at a scan rate of 4 º/min. Fourier transform infrared spectroscopy (FT-IR) was performed over the wave number range of 4000–400 cm^{-1} with a FT/IR-6100 FT-IR Spectrometer, (JASCO, Japan). The X-ray photoelectron spectroscopy (XPS, JPC-9010MC, JOEL, Japan) analysis was performed by using an unmonochromated Mg-Kα X-ray source (1253.6 eV) with vacuum better than 1×10^{-7} Torr. For the transmission electron microscopic (TEM) analysis, the samples were suspended in water/menthol (0.2 mg/ml) by ultra-sonication for 10 min and then the dispersion was drop-casted on a fresh lacey carbon TEM grid. The beam energy used for TEM analysis was 200 keV. Raman analysis was performed with Invia Raman Microscope (Renishaw, United Kingdom) with an excitation wavelength at 532 nm. The electrical conductance was tested by a four-point probe resistivity meter (Loresta EP, Model MCP-T360, Mitsubishi Chemical Co., Japan) at room temperature.

3. Results and discussion

3.1 Characteristics of the TDO-reduced graphene

In AFM images (Figure 2), the graphene oxide produced for these studies exhibited a thickness of ~1.1 nm, which indicated that the graphene oxide was exfoliated into single- or a few-layered sheets [27]. The length or breadth of each of twenty pieces of the graphene oxide was found to be around 1 –

5 micrometers. Through TEM images of the TDO-reduced graphene, we observed sheet-shaped structures with a wrinkled surface (Figure 3). In the selected area electron diffraction (SAED) pattern (Figure 3) for the TDO-reduced graphene, we observed hexagonal and dodecagonal symmetry diffractions, indicating the TDO-reduced graphene had a well crystallized structure. For the graphene oxide precursor, the oxygen-containing groups as well as defects in the crystal lattice served as strong scattering centers and blocked the π-electrons transfer (data not shown). In contrast, for the TDO-reduced graphene, the oxygen-containing groups were no longer present and also the atomic domain containing defects were converted into long-ranging extended conjugated networks in the graphitic lattice.

In the XRD patterns of the materials used in these studies (Figure 4), pristine graphite exhibited a basal reflection (002) peak at 2θ=26.44°(d spacing = 0.336 nm) due to the tightly packed layers of the graphene (Figure 4) [31]. For the synthesized graphene oxide, the 002 reflection peak shifted to the lower angle (2θ=12.14°) and the distance of graphene plates expanded to 0.728 nm. The increase in d spacing is attributed to the intercalation of water molecules and grafting with functional groups, such as hydroxyl, epoxy, and carboxyl, between the layers of graphite that occurred during oxidation [32]. For the TDO-reduced graphene, the interlayer distance returned to 0.336 nm; this again indicated that the graphene structure was restored after the removal of most of the oxygen functional groups[33]. The new broadened diffraction peak at 26.44° and reduced peak intensity demonstrate that graphene was exfoliated into single-layered or few-layered sheets, affording the formation of a new lattice structure which was significantly different from the pristine graphite. On the contrary, samples obtained using sodium hydrosulfite and L-ascorbic acid as the reductants showed only the 2.14°diffraction peak; this again indicates the poor reduction efficiency of these two reductants.

The TDO-reduced graphene samples were analyzed using FT-IR (Figure 5). The most characteristic features for the graphene oxide are the vibration and deformation bands of O-H at 3380 cm^{-1}, the stretching vibration band of C=O at 1728 cm^{-1}, and the stretching vibration bands of epoxy and alkoxy groups at 1221 and 1043 cm^{-1} [18, 34]. In addition, the aromatic C=C (1619 cm^{-1}) stretching vibrations due to the unoxidized graphitic domains and the C-H bending vibration at 1362 cm^{-1} also appeared in the spectrum. After the TDO-reduction treatment, the FT-IR peaks corresponding to the oxygen-containing groups decreased. Pristine graphite was also analyzed under identical experimental conditions, similar spectra to that for the TDO-reduced graphene were observed (data not shown).

Raman scattering spectroscopy is commonly used to characterize the structural properties of graphite, graphene oxide and graphene, including the degrees of disorder and defect, and/or the doping levels. The Raman spectrum for the pristine graphite showed a strong G band peak at 1580.8 cm^{-1} and a weak D-band peak at 1349.4 cm^{-1} (Figure 6). These two main features, the G band and D band, are attributed to the first order scattering of E_{2g} vibration mode of sp^2-bonded carbon atoms and the breathing mode of κ-point phonons of A_{1g} symmetry [35], respectively. For the graphene oxide, the G band was widely broadened and slightly shifted to 1582.7 cm^{-1} due to the isolated double bonds that resonate at higher frequencies. In contrast, the D band was shifted to a lower region at 1360.8 cm^{-1} and became more prominent, indicating the reduction in size of the in-plane sp^2 domains. After the reduction with TDO, the intensity ratio of D-band to G-band (I_D/I_G ratio) in the Raman spectrum decreased from 2.65 for graphene oxide to 1.81 in reduced graphene. For the samples obtained using sodium hydrosulfite and L-ascorbic acid as the reductants, the I_D/I_G ratios were found to be 2.03 and 2.14, respectively. The large amounts of hydroxyl, epoxy and alkoxy groups present in graphene oxide are the key groups responsible for causing the decrease in the

overall amount of the aromatic rings and as a result, diminishing the relative intensity of the G band. For the TDO-reduced graphene, the residual oxygenated groups and the numbers of the aromatic domains are both important in determining the value of I_D/I_G ratio. In the case that a reductant having a lower reduction ability was used, the reduced graphene contains larger numbers of the smaller sized graphene, thus leading to an increase in the I_D/I_G ratio. In contrast, in a case where a strong reducing agent was used, the graphene was built up by the larger sized aromatic domains and as a result, a smaller value of the I_D/I_G ratio was obtained. The I_D/I_G ratio for the TDO-reduced graphene was almost identical to that for the graphene obtained by reducing graphene oxide using N,N-dimethylhydrazine [36]; this result indicated that TDO has a reduction potential which is comparable to that of the hydrazine-based compounds.

XPS was used to evaluate the changes on C/O ratios involved in the TDO-reduction of graphene oxide (Figure 7). The C1s spectrum for the pristine graphite clearly indicated a lower binding energy feature at 284.4 eV (which is responsible for the C=C bonds), a higher binding energy feature at 285.8 eV (which corresponds to the C-C bonds) and followed by a shoulder at 286.9 eV (which is assigned to the range of C-C sp^3). The C1s XPS spectrum for the graphene oxide shows a considerable degree of oxidation with four components that correspond to carbon atoms involved in different functional groups, namely, the non-oxygenated aromatic C (C=C/C-C), the C in C-O bonds, the carbonyl C (C=O) and the carboxylate C (-COO-), centered around the binding energies of 284.4, 285.7, 287.7, and 289.4 eV, respectively[20, 37]. After the reduction using TDO, the intensities for all C1s peaks of the carbon-oxygen binding species, especially the peaks of C=O and C-O bonds, decreased rapidly, revealing that most of the oxygen containing functional groups were removed after the reduction; the C/O ratio increased from 1.84:1 to 5.89:1. In previous studies, the C/O ratio for graphene obtained using L-ascorbic acid as the reductant was increased

from 2.0:1 to 5.7:1 [38] and from 2.7:1 to 10.3:1 using hydrazine as the reductant [39]. However, the reduction with L-ascorbic acid required 48 hours while the reduction with hydrazine required 24 hours. In our method with TDO as the reductant, the reduction was accomplished within 30 minutes. The entire O1 spectrums for the graphene oxide, for the TDO-reduced graphene and for the pristine graphite were also shown in Figure 7. The O1s peak intensity at 533eV for the TDO-reduced graphene was reduced to a value similar to that of the pristine graphite. Table 1 summarizes the reduction efficiency of TDO, sodium hydrosulfite and L-ascorbic acid with C/O ratios and the electrical conductance as the indocators.

3.2 The proposed reduction mechanism

The electrical conductance is used as an indicator of the extent to which the electronic conjugation in the graphene is restored after the reduction of the graphene oxide. For evaluating the electrical conductance of the TDO-reduced graphene, graphene-based films were prepared by reduction of 0.015 mm thick graphene oxide-based films with TDO for 30 min. The electrical conductance of the graphene-based film was measured using a digital four-point probe system at room temperature. Five different sites on each film sample were measured and the results were summarized in Table 1. The average value of the electrical conductance of these graphene samples obtained by using TDO, sodium hydrosulfite and L-ascorbic acid were found to be 3.205×10^3 S m^{-1}, 8.454×10^2 S m^{-1}, 2.958×10^{-2} S m^{-1}, respectively. The value of TDO is identical with that of the electrical conductance reported for the graphene films obtained using the hydrazine vapor reduction method [40]. When TDO functioned as the catalyst under alkaline conditions, it decomposed rapidly to produce sulfoxylic acid, which is a highly effective reductant. After the reduction reaction, the sulfoxylic acid was converted into hydrogen sulfite which is also capable of reducing graphene oxide through

a two-step nucleophilic reaction and SO_4^{2-} is believed to be the final product[34, 41-43]. The change in color of the graphene oxide aqueous solution before and after the chemical reaction is visible evidence indicating that the graphene oxide was reduced into graphene. Figure 8 shows typical photographs for the graphene oxide aqueous solution and the reduced graphene sheets in aqueous solution together with the schematic illustrations regarding the changes of the functional groups possibly involved in reduction of graphene oxide with TDO.

4. Conclusions

TDO is an efficient and nontoxic reductant for the massive production of high-quality, solution-based graphene using graphene oxide as the precursor. The oxygen-containing functionalities have been eliminated and the crystalline structures of the aromatic domains have been restored into the electronic conjugation states. This green-reduction method should open a new possibility for the mass fabrication of graphene-based functional materials for numerous practical applications.

References

1 A. K. Geim, *Science* **2009**, *324*, 5934.

2 A. K. Geim, K. S. Novoselov, *Nat Mater* **2007**, *6*, 3.

3 D. A. Dikin, S. Stankovich, E. J. Zimney, R. D. Piner, G. H. B. Dommett, G. Evmenenko, S. T. Nguyen, R. S. Ruoff, *Nature* **2007**, *448*, 7152.

4 A. H. Castro Neto, F. Guinea, N. M. R. Peres, K. S. Novoselov, A. K. Geim, *Rev. Mod. Phys.* **2009**, *81*, 1.

5 S. Pei, H.-M. Cheng, *Carbon* **2012**, *50*, 9.

6 S. Stankovich, D. A. Dikin, R. D. Piner, K. A. Kohlhaas, A. Kleinhammes, Y. Jia, Y. Wu, S. T. Nguyen, R. S. Ruoff, *Carbon* **2007**, *45*, 7.

7 S. Park, J. An, J. R. Potts, A. Velamakanni, S. Murali, R. S. Ruoff, *Carbon* **2011**, *49*, 9.

8 S. Nagase, X. G. Gao, X. F., J. Jang, *J. Phys. Chem. C* **2010**, *114*, 2.

9 V. C. Tung, M. J. Allen, Y. Yang, R. B. Kaner, *Nat. Nanotech.* **2009**, *4*, 1.

10 S. Stankovich, D. A. Dikin, G. H. B. Dommett, K. M. Kohlhaas, E. J. Zimney, E. A. Stach, R. D. Piner, S. T. Nguyen, R. S. Ruoff, *Nature* **2006**, *442*, 7100.

11 S. Park, Y. Hu, J. O. Hwang, E.-S. Lee, L. B. Casabianca, W. Cai, J. R. Potts, H.-W. Ha, S. Chen, J. Oh, S. O. Kim, Y.-H. Kim, Y. Ishii, R. S. Ruoff, *Nat. Commun.* **2012**, *3*.

12 G. Wang, J. Yang, J. Park, X. Gou, B. Wang, H. Liu, J. Yao, *J. Phys. Chem. C* **2008**, *112*, 22.

13 Y. Si, E. T. Samulski, *Nano Lett.* **2008**, *8*, 6.

14 H.-J. Shin, K. K. Kim, A. Benayad, S.-M. Yoon, H. K. Park, I.-S. Jung, M. H. Jin, H.-K. Jeong, J. M. Kim, J.-Y. Choi, Y. H. Lee, *Adv. Funct. Mater.* **2009**, *19*, 12.

15 W. Gao, L. B. Alemany, L. Ci, P. M. Ajayan, *Nat. Chem.* **2009**, *1*, 5.

16 X. Fan, W. Peng, Y. Li, X. Li, S. Wang, G. Zhang, F. Zhang, *Adv. Mater.* **2008**, *20*, 23.

17 T. N. Zhou, F. Chen, K. Liu, H. Deng, Q. Zhang, J. W. Feng, Q. A. Fu, *Nanotechnology* **2011**, *22*.

18 J. Zhang, H. Yang, G. Shen, P. Cheng, J. Zhang, S. Guo, *Chem. Commun.* **2010**, *46*, 7.

19 M. J. Fernández-Merino, L. Guardia, J. I. Paredes, S. Villar-Rodil, P. Solís-Fernández, A. Martínez-Alonso, J. M. D. Tascón, *J. Phys. Chem. C* **2010**, *114*, 14.

20 J. Gao, F. Liu, Y. Liu, N. Ma, Z. Wang, X. Zhang, *Chem. Mater.* **2010**, *22*, 7.

21 T. Kuila, S. Bose, P. Khanra, A. K. Mishra, N. H. Kim, J. H. Lee, *Carbon* **2012**, *50*, 3.

22 C. A. Amarnath, C. E. Hong, N. H. Kim, B. C. Ku, T. Kuila, J. H. Lee, *Carbon* **2011**, *49*, 11.

23 Y. Liu, Y. Li, Y. Yang, Y. Wen, M. Wang, *J. Nanosci. Nanotechno.* **2011**, *11*, 11.

24 W. Chen, L. Yan, *Nanoscale* **2010**, *2*, 4.

25 W. Chen, L. Yan, P. R. Bangal, *Carbon* **2010**, *48*, 4.

26 G. K. Ramesha, S. Sampath, *J. Phys. Chem. C* **2009**, *113*, 19.

27 S. Park, R. S. Ruoff, *Nat. Nanotech.* **2009**, *4*, 4.

28 A. Lerf, H. He, M. Forster, J. Klinowski, *J. Phys. Chem. B* **1998**, *102*, 23.

29 J. Kim, L. J. Cote, F. Kim, W. Yuan, K. R. Shull, J. Huang, *J. Am. Chem. Soc.* **2010**, *132*, 23.

30 W. S. Hummers, R. E. Offeman, *J. Am. Chem. Soc.* **1958**, *80*, 6.

31 I. K. Moon, J. Lee, R. S. Ruoff, H. Lee, *Nat. Commun.* **2010**, *1*.

32 J. Shen, Y. Hu, M. Shi, X. Lu, C. Qin, C. Li, M. Ye, *Chem. Mater.* **2009**, *21*, 15.

33 S. Park, J. An, I. Jung, R. D. Piner, S. J. An, X. Li, A. Velamakanni, R. S. Ruoff, *Nano Lett.* **2009**, *9*, 4.

34 L. F. Yan, W. F. Chen, P. R. Bangal, *J. Phys. Chem. C* **2010**, *114*, 47.

35 F. Tuinstra, J. L. Koenig, *J. Chem. Phys.* **1970**, *53*, 3.

36 S. Villar-Rodil, J. I. Paredes, A. Martinez-Alonso, J. M. D. Tascon, *J. Mater. Chem.* **2009**, *19*, 22.

37 L. Sun, H. Yu, B. Fugetsu, *J. Hazard. Mater.* **2012**, *203–204*, 15.

38 X. Zhou, J. Zhang, H. Wu, H. Yang, J. Zhang, S. Guo, *J. Phys. Chem. C* **2011**, *115*, 24.

39 S. Stankovich, R. D. Piner, X. Chen, N. Wu, S. T. Nguyen, R. S. Ruoff, *J. Mater. Chem.* **2006**, *16*, 2.

40 D. Yang, A. Velamakanni, G. Bozoklu, S. Park, M. Stoller, R. D. Piner, S. Stankovich, I. Jung, D. A. Field, C. A. Ventrice Jr, R. S. Ruoff, *Carbon* **2009**, *47*, 1.

41 W. Czajkowski, *Dyes Pigment.* **1994**, *26*, 2.

42 K. Nakagawa, k. Minami, *Tetrahedron Lett.* **1972**, *5*.

43 S. A. Svarovsky, R. H. Simoyi, S. V. Makarov, *J. Phys. Chem. B* **2001**, *105*, 50.

Figures and captions

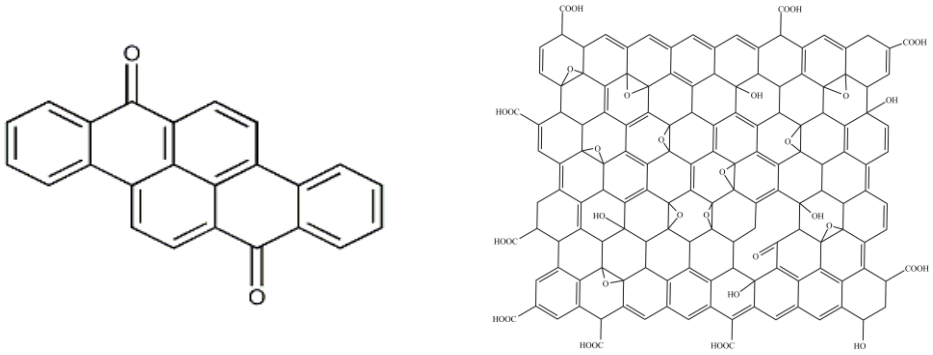

Figure 1. Schematic illustrations of the vat dye yellow 4 (left) used as a dyestuff in the textile industry and the typical structure of graphene oxide (right).

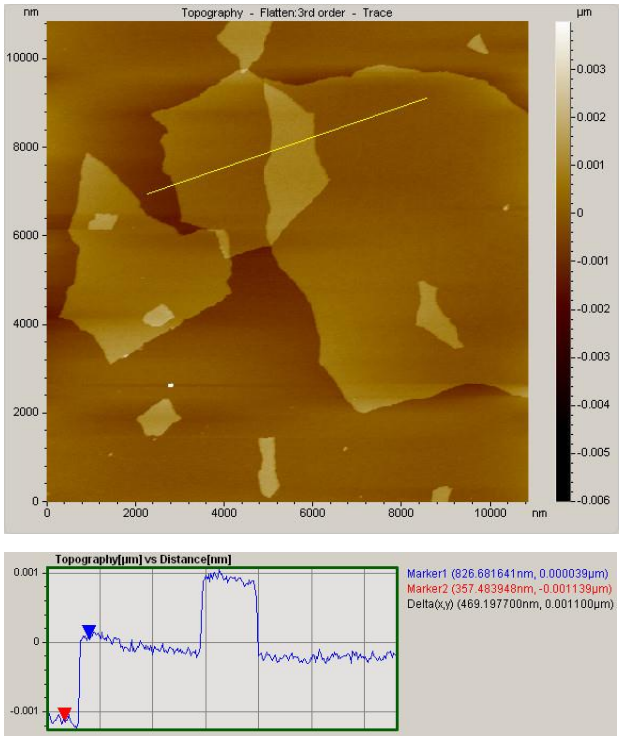

Figure 2. - A typical AFM image of the graphite oxide on a mica substrate. The thickness of the graphene oxide was estimated to be 1.1 nm.

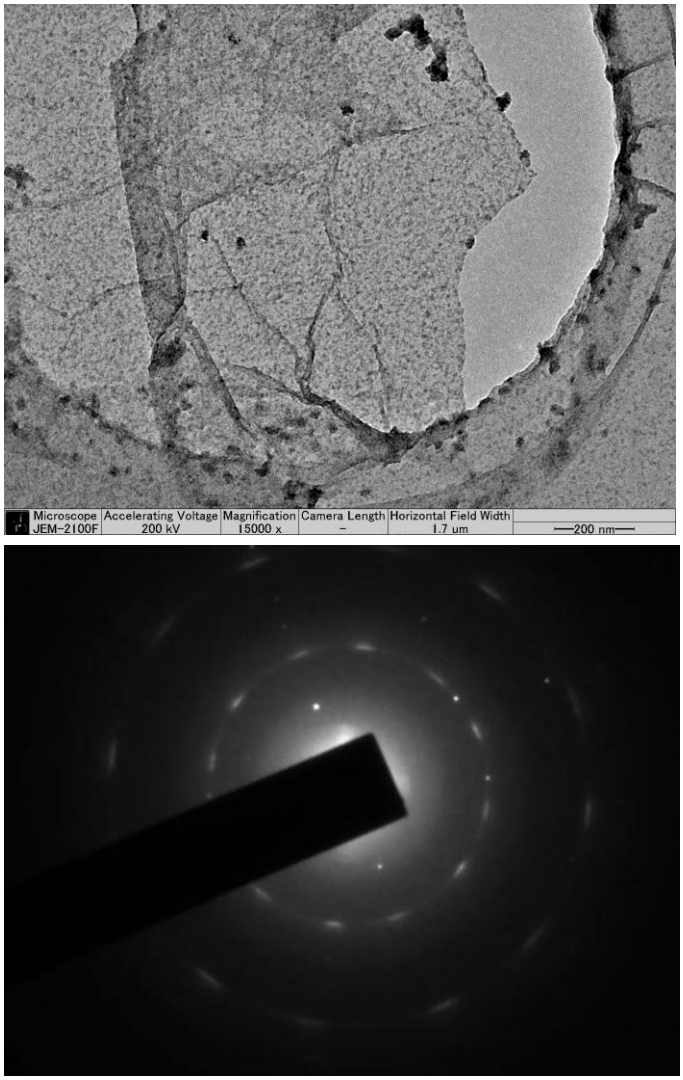

Figure 3. TEM image (up) and the relative selected area electron diffraction pattern (down) of the TDO-reduced graphene.

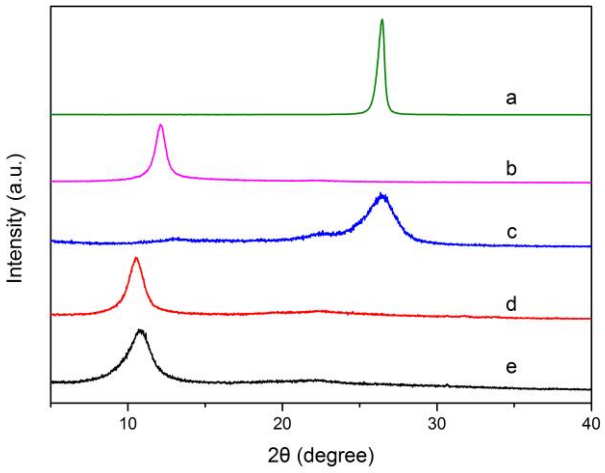

Figure 4. X-ray diffraction patterns of (a) the pristine graphite, (b) graphene oxide, (c) reduced graphene with TDO, (d) reduced graphene with $Na_2S_2O_4$ and (e) reduced graphene with L-ascorbic acid.

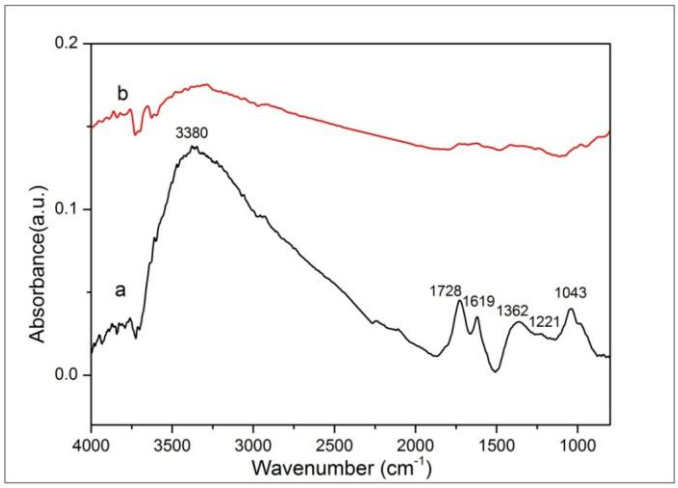

Figure 5. Typical FT-IR spectra of graphene oxide (a) and of the TDO-reduced graphene (b).

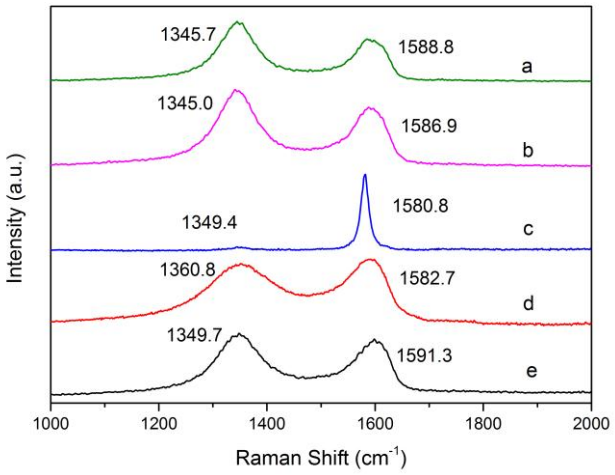

Figure 6. Raman spectra of (a) reduced graphene with $Na_2S_2O_4$, (b) reduced graphene with L-ascorbic acid, (c) graphite, (d) graphene oxide (GO) and (e) reduced graphene with TDO.

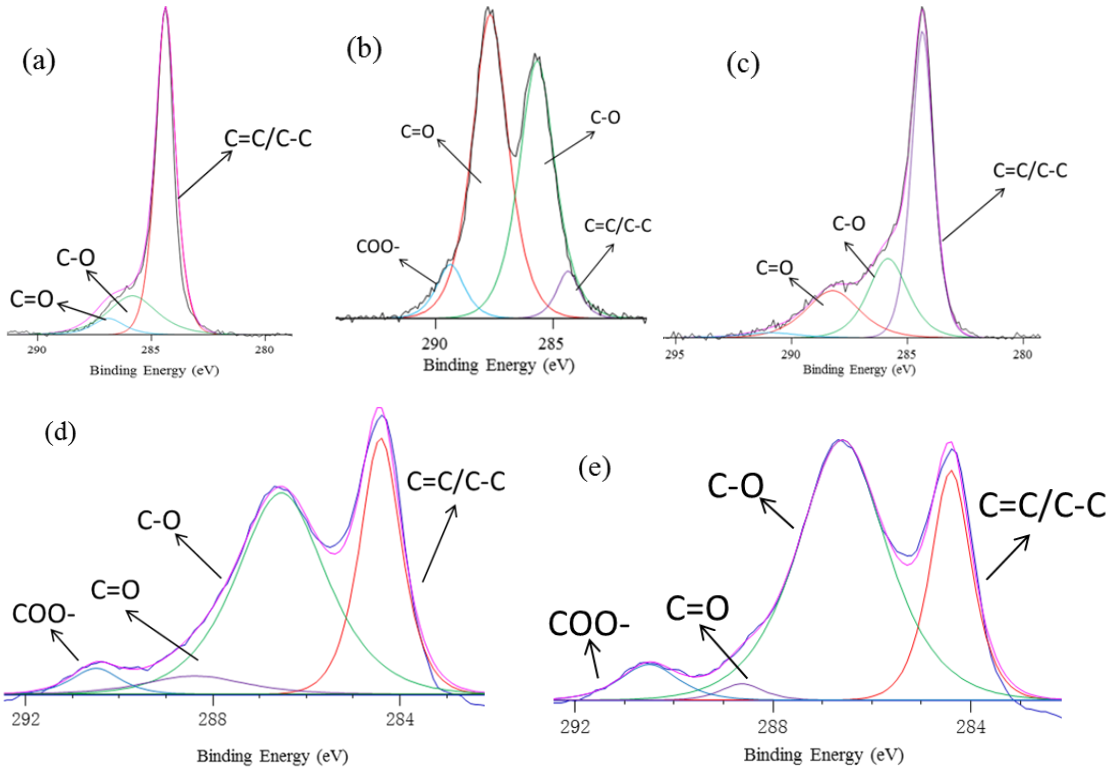

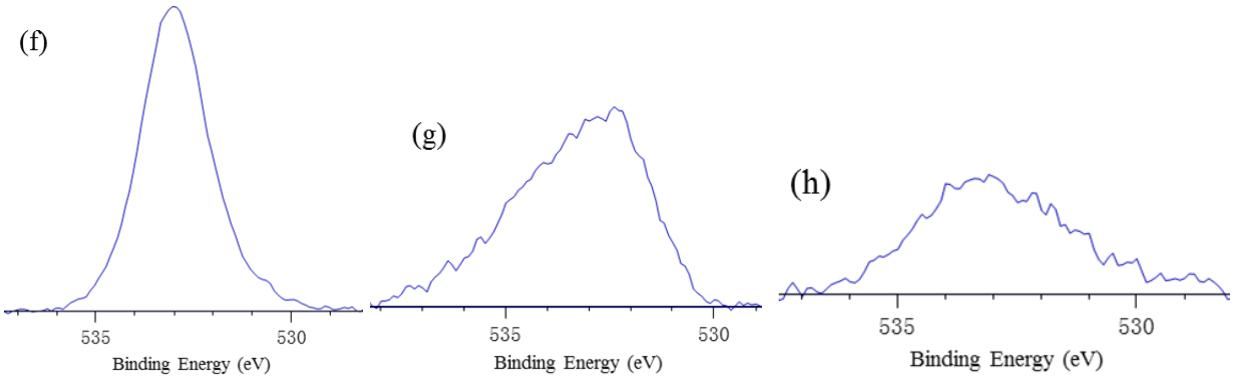

Figure 7. High-resolution XPS spectra and curve fitting of C1s spectra of (a) graphite, (b) graphene oxide, (c) TDO-reduced graphene, (d) reduced graphene with $Na_2S_2O_4$, (e) reduced graphene with L-ascorbic acid, (f) the O1s spectra of graphene oxide, (g) the O1s spectra of TDO-reduced graphene and (h) the O1s spectra of graphite.

Table 1. Comparison of the reduction efficiency of TDO, $Na_2S_2O_4$ and L-ascorbic acid.

Reductants	Reduction conditions	C/O ratios	Electrical conductance/ S m^{-1}
TDO	80 ºC/30 min	5.89:1	3.205×10^3 S m^{-1}
$Na_2S_2O_4$	80 ºC/30 min	3.67:1	8.454×10^2 S m^{-1}
L-ascorbic acid	80 ºC/30 min	3.23:1	2.958×10^{-2} S m^{-1}

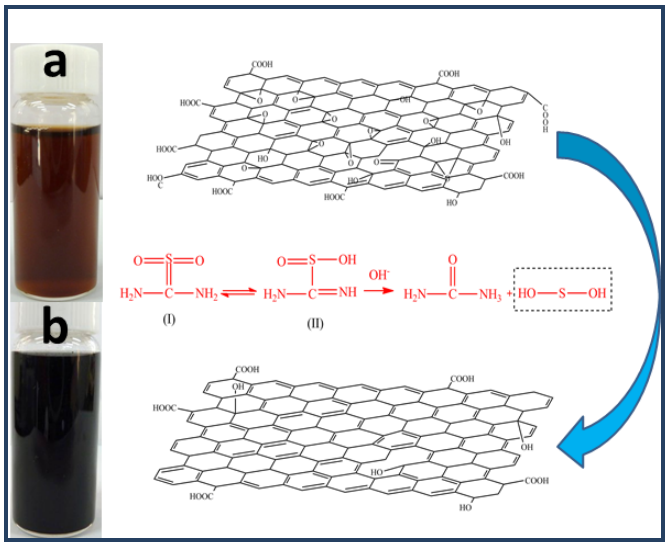

Figure 8. Schematic illustration of the reduction, including photographs of (a) the graphene oxide aqueous solution and (b) the reduced graphene sheets in aqueous solution.